

# Precision Spectroscopy of Excited States in Rubidium

CHIN Chii Tarnng

*An academic exercise presented in partial fulfilment for the degree of  
Bachelor of Science with Honours in Physics.*

Supervisor: Prof C. Kurtsiefer and G. Maslennikov

**Department of Physics**

**National University of Singapore**

**2010/2011**

# Acknowledgements

This project would not have been possible without the help and support of all the people in Professor's Christian's lab.

I would like to thank my supervisors, Professor C. Kurtziefer and G. Maslennikov, for their help and encouragement throughout the period of the project.

Special thanks to Brenda, Barath, Gurpreet and Syed for their continuous support and guidance in the technical aspect of this project, as well as patiently teaching me the theory behind the project.

And not forgetting the rest of the team who readily assist me whenever I am in need of help.

Chii Tarng

4 April 2010



# Abstract

Using laser to investigate the structure of atoms has been one of the most important applications of laser. A laser system which provides both 780nm and 776nm laser light corresponding to a 3 level transition ( $5S_{1/2}$  to  $5D_{3/2}$ ) in the energy structure of Rubidium is used in this experiment to perform a precision spectroscopy of Rubidium.

# Contents

<b>1 Introduction</b>	<b>1</b>
<b>2 Theory Considerations</b>	<b>4</b>
2.1 Two Photons Transition .....	6
2.2 Hyperfine splitting of Rubidium-87 .....	8
2.3 Doppler Broadening .....	9
2.4 Saturated Absorption Spectroscopy .....	10
2.5 PDH Locking Technique .....	14
<b>3 Experimental Setup</b>	<b>17</b>
3.1 Gas Discharge of Rubidium Vapour .....	18
3.2 Laser System Setup .....	20
3.2.1 780nm Laser Setup .....	21
3.2.2 Fiber Coupler .....	23
3.2.3 FM Spectroscopy Board .....	24
3.2.4 776nm Laser Setup .....	24



## CONTENT

<b>4 Results and Discussion</b>	<b>26</b>
4.1 Spectroscopy of 780nm Transition .....	26
4.2 Spectroscopy of 776nm Transition .....	30
<b>5 Conclusion</b>	<b>31</b>
<b>A Hyperfine Splitting</b>	<b>33</b>
<b>B Experimental Setups</b>	<b>35</b>

# Chapter 1

## Introduction

Many works have been done in pursue for attaining quantum computing. For a while now, interest has been put into investigating generation of 2 photons state via 4 wave-mixing (FWM) in an alkali metal atomic medium due to their high degree of non-linearity. Alkali metals are well studied and are known for being versatile tools for spectroscopy and nonlinear optics in atomic physics, hence making them ideal for studies of 2-photon spectroscopy [1, 2, 3].

In this work, we shall consider the use of Rubidium (Rb), particularly, one of the isotope, Rubidium-87. In  $^{87}\text{Rb}$ , the  $5S_{1/2}$  to  $5P_{3/2}$  (780nm) and  $5P_{3/2}$  to  $5D_{3/2}$  (776nm) transitions shown in Fig 1.1 are easily accessible with simple diode laser systems [4]. This

*Fig 1.1: Energy Level of Rubidium-87*

process is relatively simple and reproducible, making it a convenient source to produce photon pairs.

For a single-photon spectroscopy on  $^{87}\text{Rb}$ , all we need is a tunable diode laser system adjusted precisely to lase at 780nm. We can observe the effect of Doppler broadening in atomic spectra by performing absorption spectroscopy. However, to investigate the hyperfine structure features shown in Fig 1.1 of the atomic system, we would need to saturate the intensity of the incident to perform a

To observe the 2 photons transition from  $5S_{1/2}$  to  $5D_{3/2}$  in  $^{87}\text{Rb}$  uses much of the same equipment. In addition to the 780nm laser system, we would need another 776nm laser system. This method offers the opportunity to directly resolve the hyperfine levels of rubidium without the presence of Doppler broadening [3].

In this thesis we describe the laser system needed to perform a 2 photons transition in  $^{87}\text{Rb}$ . In Chapter 2, we shall look at the basic theory behind the works of my project. In Chapter 3, we describe the experimental setup needed to perform spectroscopy of the 2 photons transition. In Chapter 4, we present the results of the spectroscopy

and interpretation of it. Finally in Chapter 5, we summarize our findings and outline future directions.

## Chapter 2

# Theoretical Considerations

In this chapter, we explore the requirements of the laser systems to carry out the spectroscopy process. It is essential to understand the theory behind the process so that we can effectively optimize the signal obtain from the spectroscopy. Furthermore, it would also help us to analyze the results accurately.

We start with a simple analysis of the three level structure of exciting the Rubidium atoms to the  $5D_{3/2}$  and the spontaneous cascading decay back to  $5S_{1/2}$ . After which, we would discuss the hyperfine structure of the energy levels. Understanding these structures allow us to tune the lasers to the required accuracy. It is also essential for us to interpret the results of the spectroscopy.

## CHAPTER 2: THEORETICAL CONSIDERATIONS

Apart from understanding the internal energy structure of the atoms, we also have to look at the distribution of velocities of the rubidium atoms in the vapor to understand the effect of Doppler shift and hence the preparation and usage of saturated absorption spectroscopy to eliminate this problem.

## 2.1 Two Photons Transition

Electrons in rubidium atoms are found in the ground state,  $5S_{1/2}$ . Upon excitation, they would move to a higher energy state depending on the discrete energy that they received. In this experiment, we are only concern with  $5P_{3/2}$  and  $5D_{3/2}$  shown in Fig 2.1. At higher energy level,  $n$ , these electrons would decay back to the ground state,  $m$ , with rates approximately given by,

$$A = \frac{\omega_{nm}^3 |d_{nm}|^2}{3\pi\epsilon_0\hbar c^3}$$

(2.1)

where  $\omega_{nm}$  is the emission frequency,  $d_{nm}$  is the transition dipole moment,  $\epsilon_0$  is the vacuum permittivity,  $\hbar$  is the reduced Planck constant and  $c$  is the vacuum speed of light.

*Fig 2.1: Energy transition in Rubidium-87*

From equation 2.1, we can see that the rate of decay is always none zero unless  $|d_{nm}|$  is zero. Therefore once the electrons are excited to the higher energy state, they would decay spontaneously back down to the ground state via any available

## CHAPTER 2: THEORETICAL CONSIDERATIONS

transition unless  $|d_{nm}|$  is zero. Whether  $|d_{nm}|$  is zero is given by the selection rules of quantum transitions [5], where  $|d_{nm}|$  is non zero if,

$$\Delta l = \pm 1, \Delta m = 0, \pm 1 \quad (2.2)$$

From equation 2.2, we can establish that decay via the path  $5D_{3/2}$  to  $5P_{1/2}$  and back to  $5S_{1/2}$  is valid. Together with the condition to conserve linear momentum, by exciting the electron in the Rubidium atom to the  $5D_{3/2}$  state via 2 photons excitation, we would then expect a cascading decay of the electron from  $5D_{3/2}$  to  $5P_{1/2}$  and then back down to  $5S_{1/2}$ . This can be seen from Fig 2.1. This cascading decay thus produces an entangled photon pair.

## 2.2 Hyperfine Splitting of Rubidium

In atoms, hyperfine structure is the splitting of atomic energy levels into closely spaced sublevels as a result of the interaction of the nuclear magnetic moment with the magnetic field of the atomic electrons [6]. A calculation of the hyperfine structure can be found in Appendix A.

A simple way to determine the number of hyperfine levels in an energy state is given by,

$$F = I - J$$

(2.3)

to

$$F = I + J$$

(2.4)

where  $F$  is the quantum number for atomic angular momentum,  $I$  is the quantum number for nuclear angular momentum and  $J$  is the quantum number for electron angular momentum.

A rough estimate to the energy shift can be found by,

$$E_{hfs} = \frac{\alpha}{2} [F(F+1) - I(I+1) - J(J+1)] \quad (2.5)$$

where  $A$  is the magnetic hyperfine structure constant.

## 2.3 Doppler Broadening

For an atom moving with velocity,  $v$ , the relationship between the angular frequency,  $\omega$ , of laser incident on it in the laboratory frame of reference and the angular frequency,  $\omega'$ , seen in a frame of reference of the atom moving at velocity,  $v$ , is given by,

$$\omega' = \omega - k \cdot v$$

(2.6)

When the laser is incident on the atom in the opposite direction, the relative angular frequency,  $\omega''$ , is now given by,

$$\omega'' = \omega + k \cdot v$$

(2.7)

It is the component of the velocity of the atom along the axis of propagation of the laser that leads to the Doppler Effect. If the atom is at rest, the atom absorbs radiation at resonance frequency  $\omega_0$ , where  $\omega' = \omega'' = \omega_0$ .

However because atoms in a vapour follow a velocity distribution given by the Maxwell Boltzmann distribution, in experiment, the atomic vapour would thus absorb radiation over a range of frequencies other than that of the resonance. It would then

be expected that this would cause a broadening in the results that we obtain from spectroscopy. And this is known as the Doppler broadening.

## 2.4 Saturated Absorption Spectroscopy

The effect of Doppler Broadening makes it impossible to resolve finer details such as the hyperfine structure. Hence proper procedures must be taken to eliminate this effect. There can be many ways to perform Doppler Free Spectroscopy [7]. For our experiment, we shall look at saturated absorption spectroscopy.

We start by considering a laser beam travelling through a sample of atoms as shown in Fig 2.2. The attenuation of the beam as it passes through the sample of atoms is given by,

$$\frac{dI}{dz} = -n\hbar\omega\gamma_s$$

(2.8)

where  $\gamma_s$  is the scattering rate of the photons and is given by,

$$\gamma_s = \frac{\Gamma}{2} \times \frac{\bar{I}}{1 + \bar{I} + \frac{2\Delta}{\Gamma}}$$

(2.9)

where  $\Gamma$  is the linewidth of the transition,  $\Delta$  is the detuning of the frequency of the laser radiation from the atomic resonant frequency and  $\bar{I}$  is given by,

$$\dot{I} = \frac{I}{I_s}$$

(2.10)

where  $I_s$  is the saturation intensity of the laser given by,

$$I_s = \frac{\pi \hbar c \gamma}{3 \lambda^3}$$

## CHAPTER 2: THEORETICAL CONSIDERATIONS

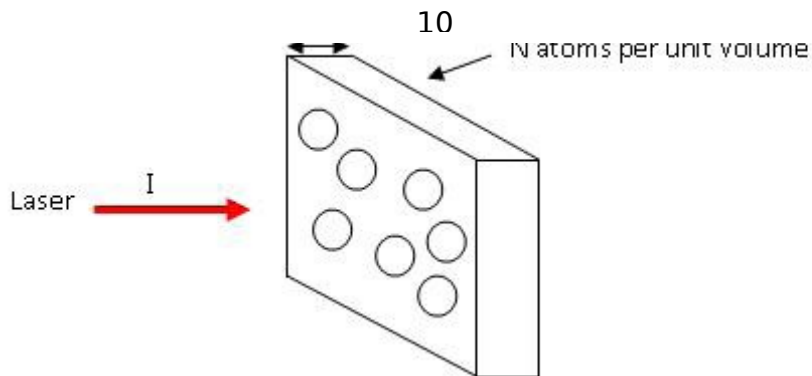


*Fig 2.2: Atoms with number density,  $N$ , distributed in a slab of thickness  $dz$ , and surface area,  $A$ .*

We look at 2 situations, when we have intensity of the laser much lower than saturated intensity, and when we have intensity of the laser higher than saturated intensity.

For the case in which intensity of the laser is lower than the saturated intensity, equation 2.8 works out to be,

$$\frac{dI}{dz} = -\alpha I$$

(2.12)

where  $\alpha = \frac{-n\hbar\omega\gamma_s}{2I_s}$ . From here, we can derive the transmission percentage to be about 0.

For the case in which the intensity of the laser is higher than the saturated intensity, equation 2.8 works out to be,

$$\frac{dI}{dz} = -\alpha$$

(2.13)

## CHAPTER 2: THEORETICAL CONSIDERATIONS

Fig 2.3: Typical setup for saturated absorption spectroscopy.

11

We can make use of the difference in transmission in these 2 cases to produce a Doppler free spectroscopy [8]. Fig 2.3 above shows a typical absorption spectroscopy setup. A strong pump beam is sent into the gas cell and a weaker probe beam (after attenuated by the gas cell) in the opposite direction is sent back into the sample. The pump beam and the probe beam are overlapped. The equations

to describe the pump beam and the probe beam are shown previously in equation 2.6 and 2.7 respectively.

Without saturating the intensity of the incident beam, we expect to see an absorption profile the shape of a Gaussian function as seen in Fig 2.4a, this is due to the velocity distribution of the atoms in the vapour. When we saturate the intensity by introducing the probe beam, the atoms which have zero velocity will absorb both the pump and the probe beam at the atomic resonance frequency,  $\omega_0$ . We also approach the case of when intensity of the laser is higher than that of the saturated intensity as seen in equation 2.13, resulting in a peak in the absorption signal at the atomic resonance

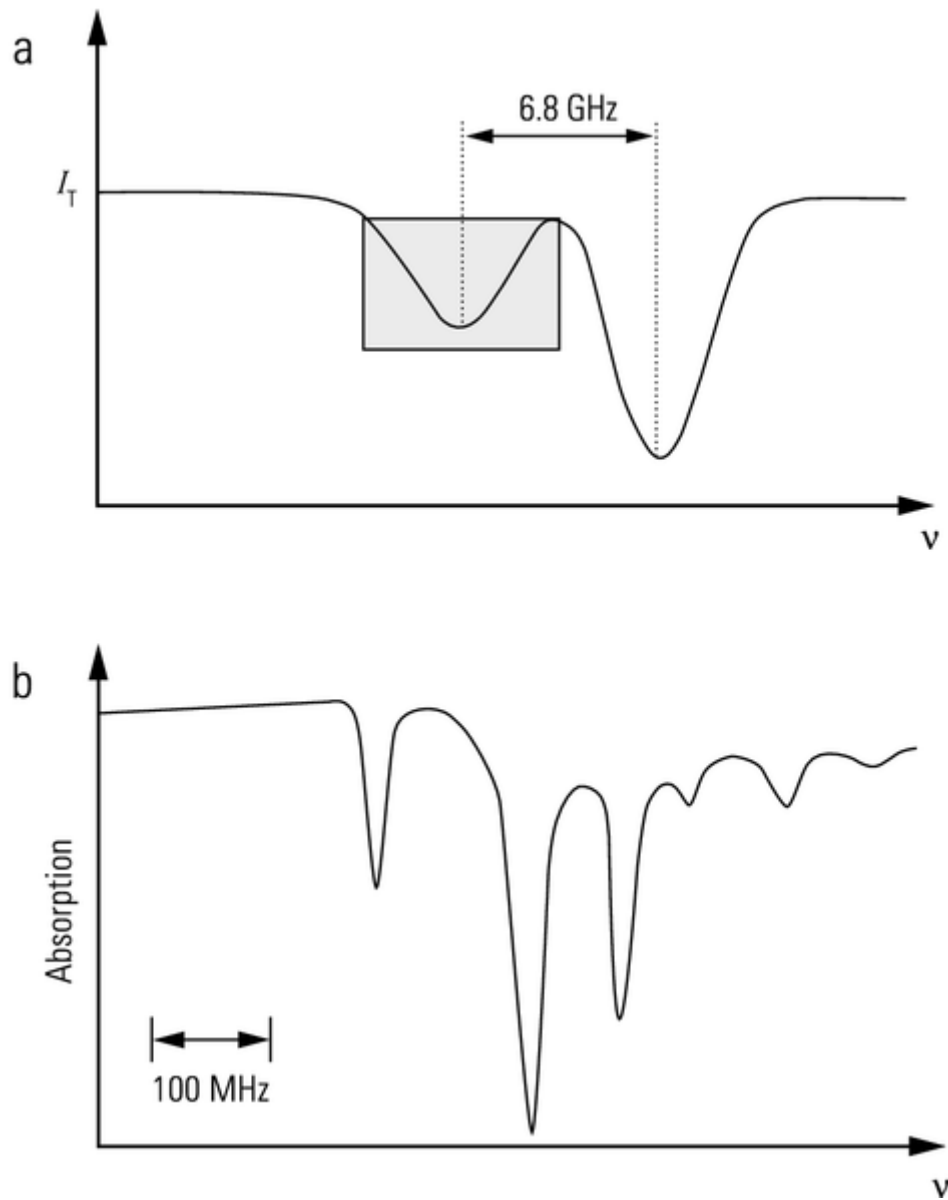


Fig 2.4: (a) Absorption profile for Rb with a non-saturated setup. (b) Hyperfine structure of one of the features from the Rb-absorption line, as measured using the saturated-spectroscopy setup

## 2.5 PDH Locking Technique

The laser is locked mechanically using the Pound-Drever-Hall (PDH) technique. Sidebands of about 20MHz are put onto the laser by an Electric Optic Modulator (EOM).

The central aspect of frequency modulation spectroscopy is the modulation of the laser frequency and its effect on the intensity of light transmitted by the gas cell [9].

The frequency at which the laser is modulated is fairly low relative to the separation of the hyperfine level. The amplitude of that modulation is also small. In this case the central laser frequency can be approximated to be periodically increasing and decreasing by a small amount. Assuming that the laser linewidth is much smaller relative to the width of the absorption, when the laser frequency is in the vicinity of an absorption line then the frequency modulation (FM) causes the absorption to modulate at the same time [9]. In this way, the laser frequency modulation is now translated onto the laser's transmitted intensity. In short, what we see here is that the frequency modulation on the laser is now converted into an amplitude modulation (AM) after the process of absorption by the atomic vapour.

## CHAPTER 2: THEORETICAL CONSIDERATIONS

With this process, the photodiode is now able to pick up information about the modulation by measuring the intensity of the beam and sending it to the FM spectroscopy board. Fig 2.5a and 2.5c demonstrates the phase relationship between the laser's FM and the absorption's AM. It can be noted by comparing Fig 2.5a and 2.5c that the conversion from FM to AM at a particular frequency depends on the slope of the absorption at that frequency [9].

By plotting the ratio of AM to FM against laser frequency, we will be able to obtain a plot similar to Fig 2.5d. The change in phase here is represented by a change in sign. This plot is known as the error signal and can be taken as the derivative of the absorption.

The polarity of the error signal can then be used to determine the direction of change of the frequency of the laser. This will then be sent to the piezoelectric element that can be use to tune the laser

## CHAPTER 2: THEORETICAL CONSIDERATIONS

*Fig 2.5: (a) Wavelength modulation is converted into amplitude modulation, giving rise to a modulation in the optical absorption of a sample at the same frequency. (b) FM to AM conversion is minimum. (c) FM to AM conversion increases again but with phase relation reversed. (d) Plot of the ratio of AM to FM versus the laser frequency, taking phases into account.*

## Chapter 3

# Experimental Setup

The aim of the setup is to excite the electrons of the rubidium atoms in the vapor to the  $5D_{3/2}$  state. To do this, we need to first populate the  $5P_{3/2}$  state. 2 methods were considered to populate the  $5P_{3/2}$  state. We can either do it by discharging the vapor in the gas cell, or by sending a laser beam locked at 780nm through the gas cell. After which, by sending a 776nm beam through the already excited rubidium vapor, we would be able to achieve the second transition.

In this chapter, we shall have a quick look into the method of discharging the vapor and then go into details for the setup of the 2 laser systems, 780nm and 776nm, and locking them to the desired wavelength.

### 3.1 Gas discharge of Rubidium Vapor

An electric circuit capable of providing high frequency and high voltage is required to discharge the rubidium vapor. A tank circuit shown in Fig 3.1 became the natural choice as we will be able to maintain high frequency and high output by supplying an input at the resonance frequency of the circuit.

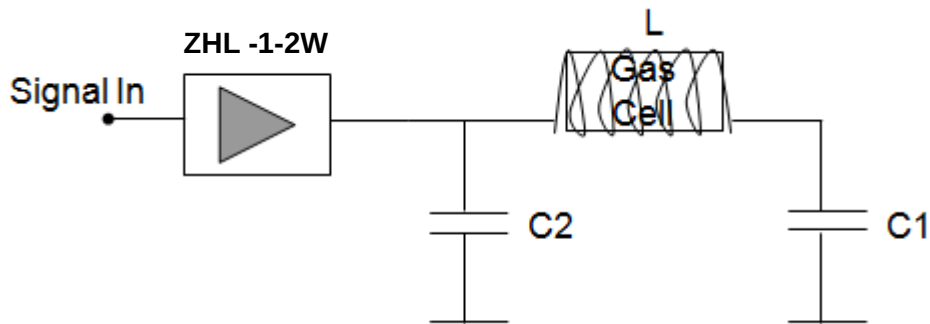


*Fig 3.1: An exciter circuit consisting of Tank Circuit and an Amplifier.*

As shown in Fig 3.1 above, the gas cell is housed in the inductor of the tank circuit. The signal input will be first amplified by the amplifier, after which, it will pass through the inductor with high voltage and high frequency, generating a strong magnetic field in the coil which will excite the rubidium atoms. Excitation of the rubidium atoms will hence provide a population at the required  $5P_{3/2}$  state. A prototype of the circuit can be seen in Appendix B.

### CHAPTER 3: EXPERIMENTAL SETUP

The circuit built could produce up to 400V across the tank circuit at the resonance frequency of 34.1MHz. However, such a process dealing with high frequency and voltage poses many technical issues such as high losses in components of the circuit.

These issues require some time to troubleshoot. Hence in view of time limitation, excitation of the rubidium atoms to the  $5D_{3/2}$  state was done via the two laser systems method.

## 3.2 Laser System Setup

*Fig 3.1: Simplified schematic diagram of the laser setup. 780nm and 776nm lasers are coupled to the gas cell at the same time for the experiment.*

The laser setup for this experiment allows 780nm and 776nm laser to be coupled and locked to a rubidium gas cell at the same time. The following section will describe how to construct and combine both systems together.

### 3.2.1 780nm Laser Setup

20

temperature (22°C), already emits at 780nm with a free-running threshold current of 36.1mA. Therefore, even though the housing of the laser diode contains a Peltier device, we do not need it to vary the temperature. The diode produces about 28.9mW at 74.1mA

In the housing of the laser diode also contains a piece of grating which can be controlled by a piezoelectric element that is

connected to the back of the grating. To optimize the power output of the diode, the grating was adjusted till the threshold current is at 31.5mA.

The laser that exits the housing is vertically polarized and the beam profile is elliptical. To make the beam circular, we make the beam pass through an anamorphic prism pair with a demagnification of 2.45. This gives the beam a circular profile with beam waist about 0.491mm. However, the anamorphic prism has a reflection coefficient for s-polarization of 0.273. Therefore, to minimise losses, a half-waveplate to make the polarization of the beam horizontal is placed in front of the anamorphic prism pair.

The beam then passes through an isolator which is effectively a Faraday rotator which rotates the polarization of the beam by about 45°. The beam then passes through another half-waveplate before a polarizing beam splitter which splits the beam into 2 parts, 1 to be coupled into the fiber coupler (to be discussed in 3.2.2), and another to pass through the EOM. The half-waveplate thus controls the power that is send into each path.

The horizontally polarized laser that passed through the PBS then goes through an in-house constructed EOM of resonant frequency 24.2MHz. The EOM is basically an optical device in which a nonlinear crystal that allows its refractive index in certain directions

to be changed is used to modulate a beam of light [10]. This is achieved by the application of an electric field. The laser is then phase modulated with the addition of 2 sidebands of  $\pm 24.2\text{MHz}$ .

The modulated beam then passes through another half-waveplate before being reflected by a PBS towards the gas cell. The half-waveplate here is then used to control the amount of power going through the gas cell to obtain the required intensity for saturated absorption spectroscopy. The saturation intensity for 780nm transition is calculated from equation 2.11 to be  $16\text{mW/cm}^2$ .

A quarter-waveplate is placed after the gas cell so that the reflected modulated beam back from the mirror after the gas cell passes through the PBS now instead of being reflected back to the input path. The reflected intensity of the modulated beam is then collected by a photodiode to be sent to a FM spectroscopy board (to be discussed in 3.2.3) to produce the error signal shown in Fig 3.2 required to lock the laser.

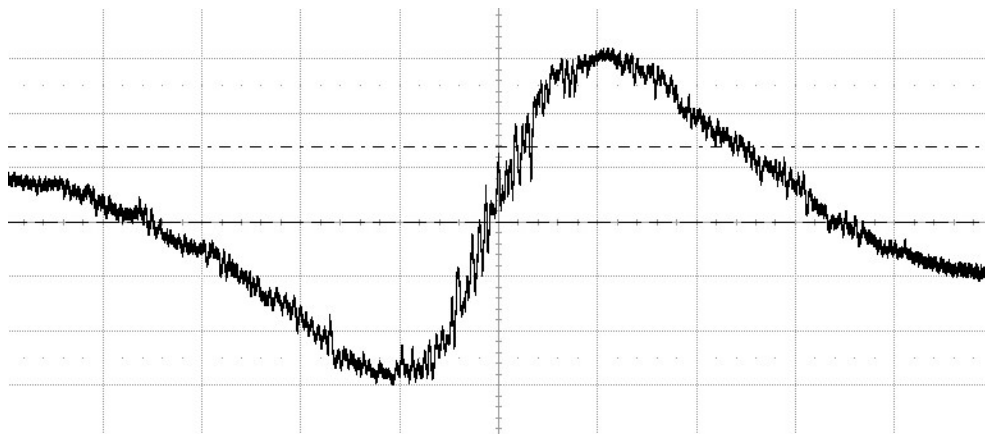


*Fig 3.2: Error Signal for the transition of  $87\text{Rb}$  from  $5S_{1/2} F=2$  to  $5P_{3/2} F=3$*

### 3.2.2 Fiber Coupler

After the first PBS in the setup, the vertically polarized 780nm laser beam will have to be coupled into the optical fiber, so that it can be introduced into the 776nm laser setup.

The beam waist as mentioned earlier is about 0.491mm, and the optical fiber used has a numerical aperture of 0.13. This requires us to use a Fiber Coupler with a lens that has a focal distance of

CHAPTER 3: EXPERIMENTAL SETUP

With the lens, we were able to get about 68% intensity of the beam into the optical fiber.

### 3.2.3 FM Spectroscopy Board

The intensity signal of the beam that goes to the photodiode will be sent to the FM spectroscopy board, where the signal will be amplified via an amplifier, MAN-1LN. The signal will then be demodulated with the local oscillator via the mixer, RPD-2. An anti-symmetric signal will then be generated and sent to the proportional-integral-derivative (PID) controller which determines and sends a voltage to the piezoelectric element at the back of the grating to adjust the wavelength of the laser [11]. A detailed schematic diagram of the board can be found in Appendix B.

### 3.2.4 776nm Laser Setup

The setup for 776nm laser system is quite similar to that of the 780nm laser system.

However, because we need the diode to lase at 776nm, we would have to control the Peltier device to lower the temperature. The Peltier device is attached to the housing that holds the diode, and is controlled by the laser diode control board. In order to obtain 776nm, we need to lower the temperature down to about 16.5°C. This is quite close to the dew point of the laboratory, hence special care was taken to ensure that the temperature do not go below 16°C during the tuning of the laser. Laser current and the grating were

adjusted instead. After several rounds of adjustment, we could obtain 776nm laser at a temperature of 17.4°C with laser current at 70.0mA.

In order to overlap the 780nm and 776nm beam in the same gas cell, we have to prepare them in different polarization, such that after passing through the cell, we can separate them using a PBS. In our setup, 776nm laser was vertically polarized and would be reflected into the photodiode after passing through the gas cell. And as for 780nm laser, it was horizontally polarized such that it passes through the PBS.

# Chapter 4

## Results and Discussion

### 4.1 Spectroscopy of 780nm Transition.

As discussed in sub-section 3.2.2, after the signal passed through the FM spectroscopy board, it will be demodulated and hence an error signal corresponding to the hyperfine levels of the energy levels can be obtained.

The gas cell used contains a mixture of  $^{85}\text{Rb}$  and  $^{87}\text{Rb}$ , thus by scanning over a range of frequency using the piezoelectric material, we can actually see a full range of error signals for both  $^{85}\text{Rb}$  and  $^{87}\text{Rb}$ . Using equations 2.3 and 2.4, we can then first determine the number of hyperfine level for both isotope at ground state,  $5S_{1/2}$ . In

## CHAPTER 4: RESULTS AND DISCUSSION

this case, because  $J$  in both isotopes is given by  $1/2$ , we expect 2 hyperfine levels for each of the ground state. For  $^{85}\text{Rb}$  ( $I=5/2$ ), we have  $F=2$  and  $F=3$ . For  $^{87}\text{Rb}$  ( $I=3/2$ ), we have  $F=1$  and  $F=2$ . This gives us 4 possible transitions to the  $5P_{3/2}$  state, one from each of the hyperfine level of the ground state shown in Fig 4.1.

*Fig 4.1 provides an illustration of the expected saturated absorption profile of the  $5S_{1/2}$  to  $5P_{3/2}$  transitions in  $^{85}\text{Rb}$  and  $^{87}\text{Rb}$ .*

That was indeed what we had observed. However for the purpose of locking the laser onto one of this transition, the transition from  $^{87}\text{Rb}$   $5S_{1/2}$   $F=2$  was chosen. Fig 4.2 shows the set of error signals for this transition. Although according to equations 2.3 and 2.4, the  $5P_{3/2}$  state of  $^{87}\text{Rb}$  should contain 4 hyperfine levels, but due

## CHAPTER 4: RESULTS AND DISCUSSION

frequency calculated (refer to Appendix A) can be used to identify the signals.

27

*transitions corresponding to the hyperfine levels of  $5P_{3/2}$  are labelled.*

It can be noted from Fig 4.2 that in between each of the identified hyperfine level, that are signals as well. These crossover

signals occur when there are several hyperfine transitions under the Doppler profile [12].

We can understand this by assuming if our laser is tuned to a frequency,  $\omega$ , exactly halfway between 2 of the hyperfine levels,  $\omega'$  and  $\omega''$ . Due to Doppler Effect, according to equations 2.6 and 2.7, atoms with speed,  $(\omega - \omega')/k$ , in the direction of the propagation of the

#### CHAPTER 4: RESULTS AND DISCUSSION

beam from  $\omega$  to  $\omega'$ . Atoms with the same speed also see a relative shift of frequency of the probe beam to  $\omega''$ . Since atoms of this velocity class are already saturated by the pump beam, the probe

28

beam will thus be able to pass through the gas cell with little decrease in its intensity. This will hence produce the error signal in between hyperfine structures.

From Fig 4.2, the 3 crossover error signals from right to left can be understood as the crossover between F=1 and F=2, F=1 and F=3, F=2 and F=3 respectively.

## 4.1 Spectroscopy of 776nm Transition.

With the transition to  $5P_{3/2}$   $F=3$  locked, the gas cell glows blue at the wavelength of 776.15746nm. This indicates the transition to  $5D_{3/2}$  state. As at  $5D_{3/2}$  state, another possible decay mode will be to decay down to  $6P_{3/2}$ , after which it will emit blue light of 420nm when it decay back down to the ground state, thus explaining the observation.

The  $5D_{3/2}$  state has 4 hyperfine levels as well. However, I should only expect to see 2 error signals corresponding to the transitions,  $5P_{3/2}$   $F=3$  to  $5D_{3/2}$   $F=2$  and  $5P_{3/2}$   $F=3$  to  $5D_{3/2}$   $F=3$ , with a estimated separation of 43.1MHz calculated by equation 2.5. The other 2 transitions are not allowed according to selection rule. I should also expect to see 1 crossover transition signal between the 2 transition signal.

Regretfully, no signal was seen as the signal was too weak. Several ways could be implemented to increase the signal strength such as heating up the gas cell. However, due to time constraint, I was unable to vary the parameters of the setup to obtain a larger signal.

# Chapter 5

## Conclusion

The basic aim of this experiment is to observe the transition of  $^{87}\text{Rb}$  from  $5S_{1/2}$  state to  $5D_{3/2}$  and perform spectroscopy on these transitions. To achieve this, 2 methods to populating the intermediate  $5P_{3/2}$  state was explored, namely, by discharging the rubidium vapour or shining a laser through the vapour cell.

Due to difficulties with technical issues, we were unable to complete the experiment for discharging the rubidium vapour. However, the exciter circuit built to provide high voltage and high frequency prove to be valid and workable. The next step would be to troubleshoot the technical issues with the circuit. Completion of the exciter circuit will prove useful to this experiment as it takes away the

## CHAPTER 5: CONCLUSION

complication of integrating 2 laser systems together and only one Doppler free spectroscopy would have to be performed.

The 2 laser systems provided the necessary means for the transitions to the  $5D_{3/2}$  state. Observation of the blue fluorescence is a clear indication that the transition was achieved. The next step to this experiment would be to vary the parameters of the setup to obtain a high enough signal that can be measured.

# Appendix A

## Hyperfine Splitting

We start with the Hamiltonian of the hyperfine structure given by,

$$H_{hfs} = \alpha (J \cdot I) + \beta \frac{[3(J \cdot I)^2 + \frac{3}{2}(J \cdot I) - I(I+1)J(J+1)]}{2I(2I-1)(2J-1)}$$

(A1)

The first term can be obtained by considering the spin-orbit term that result from the magnetic dipole interaction between the nucleus and the electron. The constant,  $\alpha$ , is called the magnetic hyperfine structure constant. The second term is obtained by considering the quadrupole moment of the nucleus. The constant,  $\beta$ , is known as the quadrupole moment of the nucleus [5].

From here, we can resolve the separation between the hyperfine levels by rewriting  $\mathbf{J} \cdot \mathbf{I}$ ,

APPENDIX A: HYPERFINE SPLITTING

$$J \cdot I = \frac{(F^2 - J^2 - I^2)}{2}$$

(A2)

Where in the eigenstate for these operators, we have,

$$J \cdot I = \frac{(F(F+1) - J(J+1) - I(I+1))}{2} = \frac{C}{2}$$

(A3)

Using the  $H_{\text{hfs}}$  to find the energy separation between the hyperfine levels, we substitute A3 into A1 to get,

$$E_{\text{hfs}} = \alpha \frac{C}{2} + \beta \frac{[3\left(\frac{C}{2}\right)^2 + \frac{3}{2}(J \cdot I) - I(I+1)J(J+1)]}{2I(2I-1)(2J-1)}$$

(A4)

A more convenient form of expression would be in terms of frequency. Where  $\alpha$  and  $\beta$  will be shifted by a constant. Using equation A4, the hyperfine structures separations of  $5P_{3/2}$  were calculated. The results compared to literature values are shown in table TA1 below.

	Separation Frequency (Calculated)	Separation Frequency (Literature)
F=1 to 2	167.1MHz	157.2MHz
F=2 to 3	258.5MHz	267.1MHz

*TA1: Calculated hyperfine frequency separation using equation A4  
against literature values.*

## Appendix B

### Experimental Setups

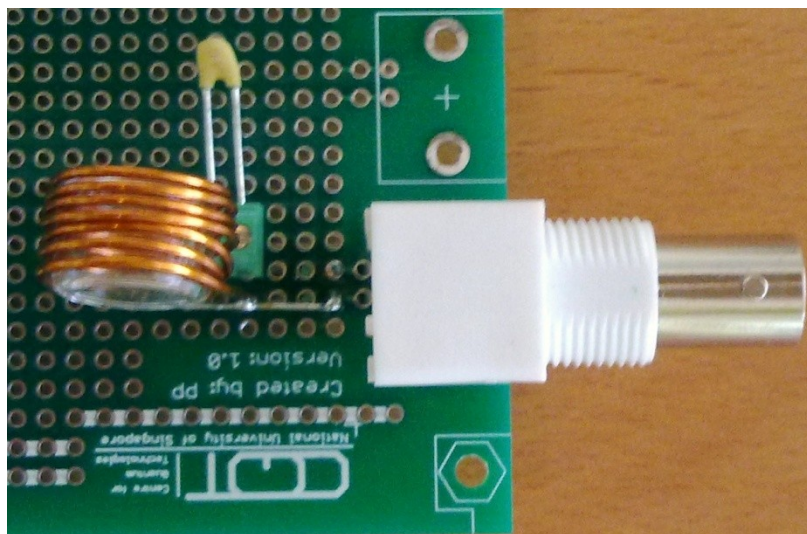


*Fig B1: A prototype of the exciter circuit.*



APPENDIX B: EXPERIMENTAL SETUPS

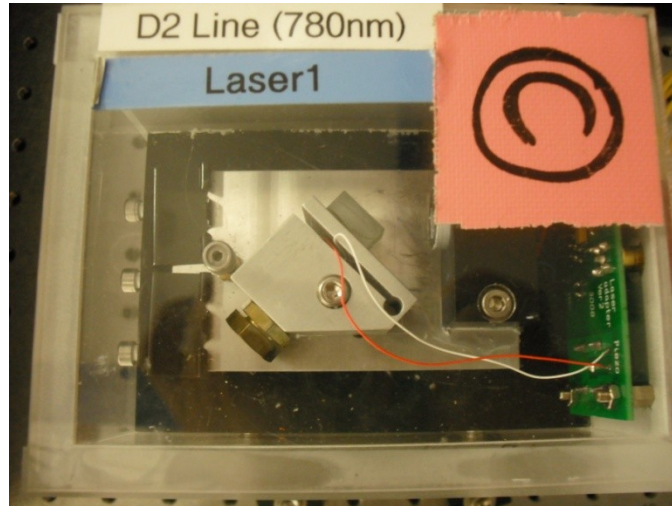
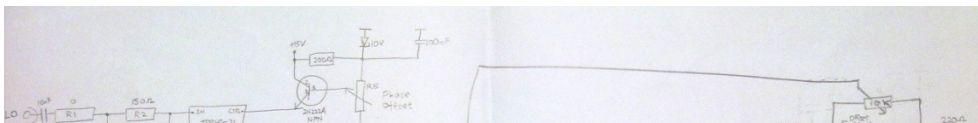


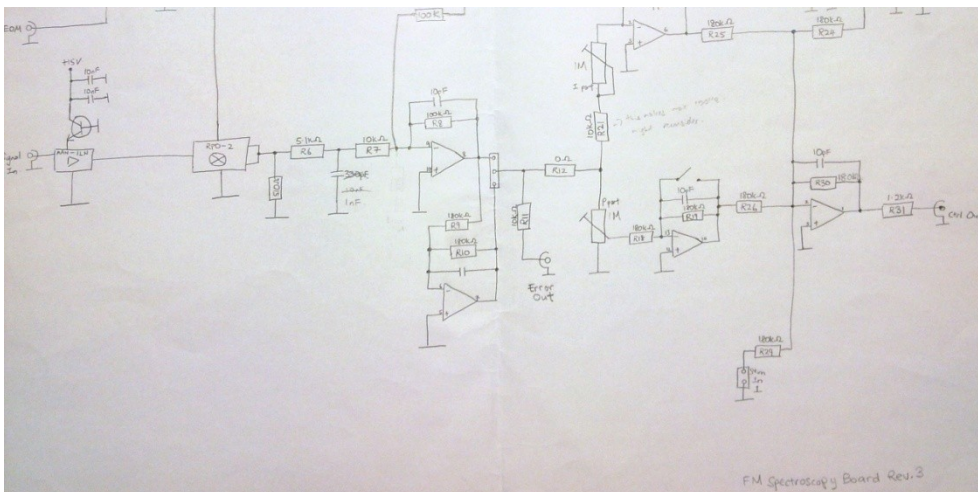
Fig B2: Diode Housing for 780nm laser diode

Fig B3: Setup of the 780nm laser system. Direction of laser is

APPENDIX B: EXPERIMENTAL SETUPS



36



*Fig B4: Schematic diagram of FM spectroscopy board Revision 3*

*Fig B5: Overlapping 780nm (blue) and 776nm (red).*

## References

- [1] F. Nez, F. Biraben, R. Felder and Y. Millerioux, "Optical frequency determination of the hyperfine components of the  $5S_{1/2}$ - $5D_{3/2}$  two-photon transitions in rubidium," *Opt. Commun.* 102, 432-438 (1993).
- [2]. M. J. Snadden, A. S. Bell, E. Riis and A. I. Ferguson, "Two-photon spectroscopy of laser-cooled Rb using a mode-locked laser," *Opt. Commun.* 125, 70-76 (1996).
- [3] A. J. Olson, E. J. Carlson and S. K. Mayer, "Two-photon spectroscopy of rubidium using a grating-feedback diode laser," *Am. J. Phys.* 74, 218-223 (2006).
- [4] A. Vernier, S. Franke-Arnold, E. Riis and A. S. Arnold, "Enhanced frequency up-conversion in Rb Vapor," *Opt. Express* 18, 17020 (2010).
- [5] Baym, *Lectures on Quantum Mechanics*, Perseus Books, (1969).
- [6] D. J. Griffiths, *Introduction to Quantum Mechanics*. Prentice Hall, (2005).
- [7] W. Demtroder, *Laser Spectroscopy*, 2nd ed., Springer-Verlag (1995).
- [8] Yifu Zhu, T.N.Wasserlauf, *Phys. Rev. A*, Vol.54, No.4, 3653, (1996).

#### CHAPTER 4: RESULTS AND DISCUSSION

[9] Newport Corporation, "FM Spectroscopy With tunable Diode Lasers," <http://www.newport.com/store/genContent.aspx/New-Focus-Application-Note-7-FM-Spectroscopy-With/979109/1033> n.d

[10] Karna, Shashi and Yeates, Nonlinear Optical Materials: Theory and Modeling, Alan (ed.) (1996).

[11] E. D. Black, Am. J. Phys. 69, 1 (2001).

[12] University of Tennessee, "FM Saturation Spectroscopy," <http://electron9.phys.utk.edu/optics507/modules/m10/saturation.htm> n.d